

Evolution of a barotropic shear layer into elliptical vortices - an inviscid Kelvin-Helmholtz instability mechanism

Anirban Guha, Mona Rahmani, and Gregory A. Lawrence

Department of Civil Engineering, University of British Columbia, Vancouver, Canada V6T 1Z4.

(Dated: June 17, 2022)

Barotropic shear layers, on becoming unstable, produce the well known Kelvin-Helmholtz instability (KH). The nonlinear manifestation of KH is usually in the form of spiral billows. However, a piecewise linear shear layer produces a different type of KH characterized by elliptical vortices connected via thin braids. Using DNS and Contour Dynamics, we investigate the role of vorticity waves in this KH formation, the rotation and nutation of the vortex, and the oscillation and straining of the braids. Our analyses answer how and why elliptical vortices like Meddies appear in nature.

Barotropic shear layers are ubiquitous in the atmosphere and oceans. These layers can become hydrodynamically unstable, giving rise to an instability mechanism widely known as the Kelvin-Helmholtz instability (KH). The non-linear manifestation of KH is usually in the form of spiralling billows, breaking of which generates turbulence and subsequent mixing in geophysical flows.

In theoretical and numerical studies, the hyperbolic tangent velocity profile is often considered to be the prototype of smooth barotropic shear layers [1]. Initially interested in understanding the long time evolution of KH emanating from this profile, we have performed a moderate Reynolds number Direct Numerical Simulation (DNS); see Fig. 1(a). The flow re-laminarizes once the KH billow completely breaks down into smallest scales via turbulent processes. At this stage the shear layer is much wider and sharper than the initial profile, and closely represents the piecewise linear profile (Fig. 1(b,c)):

$$U(z) = \begin{cases} 1 & z \geq 1 \\ z & -1 \leq z \leq 1 \\ -1 & z \leq -1 \end{cases} \quad (1)$$

Here U is the non-dimensional velocity of the shear flow. Eq. (1) now becomes the new base flow and serves as the initial condition for the subsequent instability processes.

The linear stability analysis of the base flow given by Eq. (1) dates back to Rayleigh [2]. However, the non-linear analysis was performed more than a century later. Using a boundary integral method known as *Contour Dynamics* (CD), Pozrikidis and Higdon [3] showed that the above-mentioned flow evolves into nearly elliptical patches of constant vorticity - the *Kirchhoff vortices*. Thus we infer that the initial shear layer profile determines the asymptotic form of the ensuing KH - smooth shear layers give rise to spiral billows, while sharp shear layers produce Kirchhoff vortices. Although the former type of KH has been thoroughly investigated in the past (in fact, spiral billow shape has traditionally been the signature of KH) [4], little is known about the non-linear evolution of the latter. This is because the sharp profile is usually considered to have little practical relevance, hence its usage is restricted to theoretical studies - mainly as a crude approximation of smooth shear layers [5, 6]. On the contrary, our DNS result in Fig. 1(a,b) indicates that

the sharp profile is also likely to occur in nature. The fact that this profile produces elliptical vortices further substantiates our claim, since such structures are well observed in geophysical and astrophysical flows, e.g. Meddies in Atlantic ocean [7] and coherent vortices in the atmosphere of giant planets [8]. Therefore it is worthwhile investigating this little known KH evolution process.

Rayleigh's [2] linear stability analysis of Eq. (1) shows it to be unstable for the range of wavenumbers $0 \leq \alpha \leq 0.64$, the fastest growing mode being $\alpha_{crit} = 0.4$. An advantage of the piecewise linear profile is that the linear instability mechanism can be interpreted in terms of interacting vorticity waves [6, 9–12]. We refer to it as the Wave Interaction Theory (WIT). This theory provides the physical reason behind the instability process, which makes it more intuitive and insightful than the conventional eigenvalue approach. From Eq. (1) we find the vorticity $\Omega \equiv dU/dz$ to be discontinuous at $z = \pm 1$. This setting allows each of these two locations to support a *stable*, progressive, interfacial wave called the vorticity wave, also known as the Rayleigh wave [6]. In rotating frame, its analogue is the Rossby edge wave which exists at sharp transitions in Potential Vorticity [11]. These two linear vorticity waves are shown in Fig. 1(d), and are mathematically expressed as follows:

$$\eta^+ = a_0 \cos(\alpha x - \Phi) \quad \text{at } z = 1 \quad (2)$$

$$\eta^- = a_0 \cos(\alpha x) \quad \text{at } z = -1 \quad (3)$$

The wave amplitude $a_0 \ll 1$ and the phase-shift $\Phi \in [-\pi, \pi]$. WIT explains how the interaction of these two monochromatic waves traveling in *opposite* directions gives rise to the linear instability process which finally leads to modal growth [6]. This happens *only* when the two waves attain a phase-locked state, the value of the phase-shift being $\Phi^{modal} = \cos^{-1}\{(1 - 2\alpha)e^{2\alpha}\}$. For $\alpha = \alpha_{crit}$, the corresponding $\Phi_{crit}^{modal} = 0.353\pi$.

Unfortunately, the promising idea of WIT is limited to the *linear* regime only. The current methodology does not allow a straightforward non-linear extension. This is a direct consequence of linearization; it forces the vorticity interfaces to become vortex sheets [9, 12]. Thus, whether *non-linear* KH can be understood in terms of two interacting non-linear vorticity waves is currently questionable. We have been able to settle this issue in this paper.

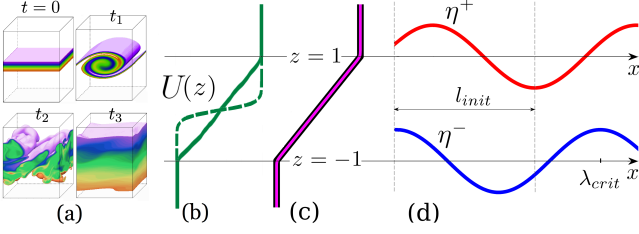


FIG. 1. (a) 3D DNS at $Re = 1200$ performed to capture the complete turbulent dissipation of a KH billow ensuing from an initial flow given by $U(z) = \tanh(z)$. (b) The dashed line represents the initial velocity profile, while the solid line shows the velocity profile once the flow re-laminarizes ($t = t_3$). (c) The Magenta line is the continuous velocity profile obtained from Eq. (5), while the thick black line below it is the piecewise linear profile from Eq. (1). Both of them closely mimic the solid green line. (d) Linear vorticity waves (exaggerated) existing at the vorticity discontinuities.

Probably the only tool capable of capturing the non-linear evolution of the profile in Eq. (1) is Contour Dynamics. CD is only applicable to flows which are inviscid, incompressible and 2D. Although the conditions seem too restrictive, they are often justifiable in geophysical and astrophysical context. In this idealized setting, the vorticity as well as the area of an arbitrary vortex patch are conserved quantities [5]. The contour (vortex patch boundary) is basically a vorticity jump and a material surface [13]. Substantial simplification is possible for constant vorticity patches; its evolution can be computed by simply solving the contour motion. This reduces the 2D problem to a 1D boundary integral. Numerically, it is done in a Lagrangian framework by tracing the contour with a set of N marker points. This methodology is known as Contour Dynamics. Realizing that the piecewise linear shear layer can be represented by a horizontally periodic patch of constant vorticity, Pozrikidis and Higdon [3] applied CD technique to solve it. The evolution of the i -th Lagrangian marker is given by [5] :

$$\frac{d\mathbf{x}_i}{dt} = -\frac{\Omega}{4\pi} \int_C \ln \left[\cosh(\alpha \Delta z'_i) - \cos(\alpha \Delta x'_i) \right] d\mathbf{x}' \quad (4)$$

where $\Omega = 1$, $\mathbf{x} = [x, z]^T$, $\Delta x'_i = x_i - x'_i$, $\Delta z'_i = z_i - z'_i$ and C is the contour around one patch. On perturbing the contour with sinusoidal disturbances, the shear layer rolled up producing nearly elliptical patches of constant vorticity [3]. This observation has allowed us to infer that *the contour is not just a material boundary, it is actually a pair of interacting vorticity waves*. This means that CD of a piecewise linear shear layer provides the right framework for simulating *non-linear* vorticity wave interactions. In other words, CD acts like a non-linear extension of WIT, thereby making it possible to understand the non-linear evolution of KH in terms of two interacting non-linear vorticity waves.

We perform a CD simulation with initial condition based on WIT; we choose $\alpha = \alpha_{crit}$ and $\Phi = \Phi_{crit}^{modal}$, and

initialize the problem using Eqs (2)-(3). This allows us to simulate the non-linear evolution of the fastest growing mode of KH arising in a piecewise linear shear layer. We consider a domain one wavelength ($\lambda_{crit} \equiv 2\pi/\alpha_{crit} = 5\pi$) long and solve Eq. (4) using central differencing for space derivatives and 4th order Runge-Kutta for time.

Previous studies have mainly used CD as a tool for *qualitative* understanding of problems on inviscid vortical flows [14]. In order to demonstrate its quantitative capabilities, we validate our CD simulation against a pseudo-spectral Direct Numerical Simulation (DNS) [15]. Moreover, DNS also provides a parallel understanding of the phenomena. We consider a domain of length λ_{crit} and carry out a 2D simulation at Reynolds number $Re = 10,000$ ($Re = 1/\nu$, ν is the viscosity). At such high Re , DNS gives a good representation of CD. Our simulation is resolved using 2880×3456 points, which is fine enough to simulate the smallest scales of the 2D flow. Since non-differentiable profiles like Eq. (1) cause Gibbs phenomena, we use a smooth velocity profile that resembles piecewise accurately; see Fig. 1(c). This profile is derived from a vorticity distribution having the form

$$\Omega(z) = \frac{1}{2} \left[1 - \tanh \left(\frac{z^2 - 1}{\epsilon} \right) \right] \quad (5)$$

By integrating Eq. (5), the velocity profile is obtained directly: $U = \int \Omega dz$. The linear stability characteristic of this profile matches almost exactly with piecewise, and has the same α_{crit} . The value of ϵ is computed by equating the total circulation of DNS with CD, producing $\epsilon = 0.100$. The vorticity field in DNS is initially perturbed to match the initial wave amplitude growth in CD.

The non-linear evolution of KH is depicted in Fig. 2. It shows the vorticity field from DNS and contour lines from CD. Vorticity of the region enclosed by the contour lines is conserved in CD. However the presence of viscosity makes this conservation invalid in DNS. By implementing high Re DNS, we minimize viscous effects, thereby making DNS comparable to CD. The basic premise behind our simulations is the conservation of total circulation $\Gamma = \Omega A$ (where vorticity $\Omega = 1$ and A is the shear layer area) and comes from Kelvin's Circulation theorem [13]. Its corollary is the conservation of shear layer area - this quantity remains fixed at its initial value $A = 2\lambda_{crit}$.

The time evolution of the wave amplitude, a , is shown in Fig. 3. The maximum shear layer height also evolves in a similar fashion since it is given by $H = 2(1 + a)$. We find the initial phase of amplitude growth to be exponential, at least for $t \lesssim 20$. Vorticity wave interaction causes the shear layer to grow non-linearly. This phenomenon leads to roll-up and formation of the elliptical core vortex (Kirchhoff vortex). The evolution process is shown in Fig. 2. The length of the domain initially between the crest of lower wave and the trough of upper wave gives rise to the elliptical core, this length being $l_{init} = (1 + \Phi_{crit}^{modal}/\pi)\lambda_{crit}/2$; see Fig. 1(d). Thus linear theory provides an estimate of the *initial* size of the KH core. The state when the core becomes completely

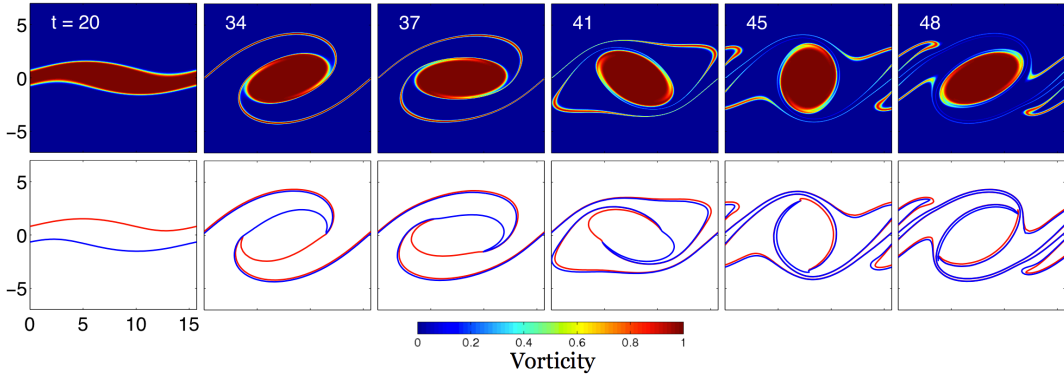


FIG. 2. Time evolution of Kelvin-Helmholtz instability - comparison between DNS (top) and CD (bottom).

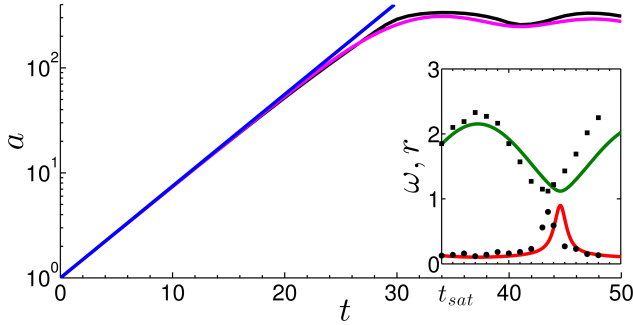


FIG. 3. Temporal variation of wave amplitude, a . The blue line is the prediction from linear theory, the black line from CD while the magenta from DNS. The inset shows the variation of ellipse aspect ratio r (green line) and angular rotation rate ω (red line) with time, obtained by solving Eqs. (6)-(7). The black markers indicate data points measured from DNS.

formed is called *saturation*, and it occurs at $t_{sat} = 34$. During saturation $\sim 80\%$ of Γ gets concentrated in the core and remains constant thereafter. Saturation is also characterized by a and H reaching maxima, the latter value being $H_{max} = 8.7$. The cores are connected by thin filaments of fluid called *braids*. They wrap around the rotating core, producing a complex spiral like structure.

The next phase of KH life cycle, from $t_{sat} < t \lesssim 50$, is the early post-saturation phase. During this phase, the core rotates with an angular velocity ω and causes the wave amplitude to oscillate with a time period $T_{amp} \approx 13$; see Fig. 3. This phase also shows another very interesting dynamics - the oscillation of the core aspect ratio r . This phenomenon is called *nutation* and is apparent from both Figs. 2 and 3. To better understand this process, we consider the simple model proposed by Kida [16]. Here, an isolated Kirchhoff vortex rotates in the presence of a constant background strain-rate γ . This strain-rate imposes a velocity field $u_s = \gamma\sigma$, $w_s = -\gamma\xi$ where σ and ξ are the Principal axes with the origin at the center of the ellipse. In our case this field mimics the leading order straining effect induced by the rotation

of other Kirchhoff vortices, whose presence gets included through the periodic boundary condition. Let the clockwise angle between σ and the ellipse major axis be θ at any instant. Then θ and r evolve as follows [16]:

$$\omega \equiv \frac{d\theta}{dt} = -\gamma \left(\frac{r^2 + 1}{r^2 - 1} \right) \sin(2\theta) + \frac{\Omega r}{(r + 1)^2} \quad (6)$$

$$\frac{dr}{dt} = 2\gamma r \cos(2\theta) \quad (7)$$

Eq. (7) clearly implies that strain causes nutation. It also reveals that the extreme positions occur at $\theta = \pm\pi/4$. Simultaneously, Fig. 2 shows that the core nutates with r being maximum along x axis and minimum along z axis. Combining these information, we get the orientation of the Principal axes - the σ axis makes an angle of $\pi/4$ with the x axis. We observe that this angle is same as that made by the braid with x axis at the stagnation point(s). This is because the braid aligns itself with the streamlines. To answer why the Principal axes have this particular orientation, we consider an ideal problem where an infinite number of Kirchhoff vortices, each having a circulation $\Gamma_{core} = \Gamma$ (note $\Gamma = 2\lambda_{crit}$), are placed along the x axis with a constant spacing λ_{crit} between their centers. Noting that the effect of a vortex patch at a point outside its boundary is same as that of a point vortex of equivalent strength placed at the patch center [5], we can easily understand how a single patch is strained by the rotation of other distant patches. It is straightforward to show that this ideal strain-rate is given by

$$\gamma' = \frac{\Gamma_{core}}{2\pi\lambda_{crit}^2} \sum_{n=-\infty, n \neq 0}^{\infty} n^{-2} = 0.067 \quad (8)$$

The Principal axes of this strain field, just like an array of point vortices, make angles of $\pm\pi/4$ with the x axis. Hence, this ideal strain field and the strain field of our actual problem have the same orientation. Before comparing the magnitudes of these two fields, it is important to note that the presence of the braids complicate the actual problem by making the strain-rate magnitude vary spatially. We simplify the analysis by assuming a

strain field of constant magnitude acting on the elliptical core, thereby reducing the problem to the Kida problem described by Eqs. (6)-(7). DNS is used to supplement the analysis by providing the values of r and θ wherever necessary. By applying this methodology, the magnitude of the actual strain-rate is found to be $\gamma = 0.073$, quite close to the ideal value of 0.067 obtained from Eq. (8).

We also capture the evolution of r and ω by solving Eqs. (6)-(7); see Fig. 3. The initial values are obtained from DNS, and $\gamma = 0.073$. The spike in ω at $t \approx 45$ is associated with $r \rightarrow 1$. Data points measured from DNS when compared with the theory reveal that the latter provides reasonably good predictions. The nutation period is found to be $T_{nut} \approx 13$, while the period of core rotation $T_{core} = 2\pi/\bar{\omega} \approx 26$ (overbar denotes average). Evidently, T_{core} is twice the value of T_{nut} as well as T_{amp} . The former is simply because one rotation corresponds to passing the coordinate axes twice; the latter is due to the braids being connected at the two ends of the core.

From Fig. 2, we find the smallest length scales to occur in the braid region adjacent to the core. This is due to the straining effect of the rotating core which causes that region to thin exponentially fast. In real flows, when a fluid element becomes sufficiently thin, the balance between strain-rate and viscous dissipation determines the small length scales. Here we estimate this local strain-rate γ_{loc} by replacing the core with a point vortex of equivalent strength and located at the core center: $\gamma_{loc} \sim \Gamma_{core}/2\pi l^2 = 0.5$, where l is a characteristic length of the core. Viscous dissipation for purely straining flows is given by $\epsilon = 4\nu\gamma_{loc}^2$ [4]. Using it in the definition of Kolmogorov length scale, $L_K \equiv (\nu^3/\epsilon)^{1/4}$, we find $L_K = (\nu/2\gamma_{loc})^{1/2}$. Since in our case γ_{loc} is the strain-rate induced by the large scale (the core), L_K is actually a Taylor microscale. Substituting the values of γ_{loc} and ν , we get $L_K \sim Re^{-1/2}$. It is worth mentioning that the magnitude of L_K is comparable to that occurring in 2D, isotropic, fully developed turbulence, this value being $\sqrt{6}Re^{-1/2}$. In order to estimate the time when Taylor microscale actually appears in our flow, we formulate a braid evolution equation similar to Eq. (2.8) of ref [17]:

$$\delta^2(t^*) = \delta^2(0) e^{-2\gamma_{loc}t^*} + \frac{\pi}{2\gamma_{loc}Re} \left(1 - e^{-2\gamma_{loc}t^*}\right) \quad (9)$$

Here $\delta(t^*)$ is the braid thickness adjacent to the core at

time $t^* = t - t_{sat}$. We estimate $\delta(0)$ from DNS and solve Eq. (9). It is found that Taylor microscale appears soon after saturation, around $t^* \approx 4$. Thus, our analysis shows that even transitional flows like KH can give rise to such small scales at quite early stages.

During the late post-saturation phase ($t \gtrsim 50$), the core surface develops progressive vorticity waves, known as Love m -waves (m is the eigenmode). In the absence of background strain, $r < 3$ is the condition for stability of a Kirchhoff vortex [13]. Although r satisfies this condition in our case, the presence of strain adds instability. The core develops unstable, finite amplitude $m = 4$ waves evolving into winding filaments, dynamics of which has been investigated in the past [18].

Finally, we emphasize on the practical relevance of this little known form of KH. Its signature, the elliptical core, is a common feature in geophysical flows, e.g. Mediterranean eddies or *Meddies*. These are massive elliptical vortices of Mediterranean origin found in the Atlantic ocean. The genesis of Meddies is highly speculative, one possible explanation being the interaction of Rossby edge waves, and is corroborated by observations near Portimão Canyon and Cape St. Vincent [7]. Noting that Rossby edge waves are analogous to vorticity waves, we infer that the evolution process of Meddies and KH formation from sharp shear layers bear a strong similarity. Moreover, our analysis (see Fig. 2 for $t \geq t_{sat}$) also justifies the typical length of the Meddies, which is approximately half of the most unstable wavelength of the Rossby edge waves [7].

Conclusion: KH ensuing from a (nearly) inviscid sharp shear layer has been investigated. This shear layer evolves into Kirchhoff vortices connected by thin braids. We study different phenomena arising in the evolution process, viz. wave interaction, wave amplitude oscillation, nutation and Taylor microscale production. Moreover, by finding and exploiting the link between two quite different theories, viz. Wave Interaction Theory and Contour Dynamics, we show that even the non-linear evolution of KH occurs through vorticity wave interactions. Our analyses provide useful insight towards understanding the formation and evolution of certain elliptical vortices arising in geophysical flows, e.g. Meddies in the Atlantic.

Thanks to Neil Balmforth and Jeff Carpenter for their helpful suggestions, Kraig Winters for the DNS code and WestGrid for providing computation support.

[1] P. Hazel, *J. Fluid Mech.* **51**, 39 (1972)
[2] J. Rayleigh, *Proc. Lond. Math. Soc.* **12**, 57 (1880)
[3] C. Pozrikidis and J. J. L. Higdon, *J. Fluid Mech.* **157**, 225 (1985)
[4] M. Rahmani, *Kelvin-Helmholtz instabilities in sheared density stratified flows*, Ph.D. thesis, The University of British Columbia, Vancouver (October 2011)
[5] C. Pozrikidis, *Introduction to Theoretical and Computational Fluid Dynamics*, first edition ed. (Oxford University Press, 1997)
[6] J. R. Carpenter, E. Tedford, E. Heifetz, and G. Lawrence, *Appl. Mech. Rev.* (to be published) (2012)
[7] L. M. Chérubin, N. Serra, and I. Ambar, *J. Geophys. Res.* **108**, 3058 (2003)
[8] J. Liu and T. Schneider, *J. Atmos. Sci.* **67**, 3652 (2010)
[9] J. Holmboe, *Geophys. Publ.* **24**, 67 (1962)
[10] F. P. Bretherton, *Q. J. Roy. Meteor. Soc.* **92**, 335 (1966)
[11] B. Hoskins, M. McIntyre, and A. Robertson, *Q. J. Roy.*

Meteor. Soc. **111**, 877 (1985)

[12] P. Baines and H. Mitsudera, J. Fluid Mech. **276**, 327 (1994)

[13] P. Saffman, *Vortex Dynamics*, first edition ed. (Cambridge University Press, 1995)

[14] D. I. Pullin, Annu. Rev. Fluid Mech. **24**, 89 (1992)

[15] K. Winters, J. MacKinnon, and B. Mills, J. Atmos. Ocean. Tech. **21**, 69 (2004)

[16] S. Kida, J. Phys. Soc. Jpn. **50**, 3517 (1981)

[17] G. M. Corcos and F. S. Sherman, J. Fluid Mech. **73**, 241 (1976)

[18] D. G. Dritschel, J. Fluid Mech. **210**, 223 (1990)